Low-temperature phase transition of a crystal in the lithium sodium niobate system

W. L. Zhong, P. L. Zhang, and H. S. Zhao
Department of Physics, Shandong University, Jinan 250100, China

Z. H. Yang, Y. Y. Song, and H. C. Chen
Institute of Crystal Materials, Shandong University, Jinan 250100, China
(Received 5 February 1992; revised manuscript received 24 June 1992)

We have studied a crystal of composition $Li_{0.03}Na_{0.97}NbO_3$ that undergoes a first-order ferroelectric-ferroelectric phase transition at about 180 K on cooling and near 260 K on heating. Evidence of the phase transition comes from anomalies in the dielectric constant, dc electrical resistivity, pyroelectric coefficient, spontaneous polarization, specific heat, and thermal expansion. X-ray-diffraction data reveal that the room-temperature phase is orthorhombic with space group $Pc2_1b$ (C_{2v}^5) and the low-temperature phase is rhombohedral with space group $R3c$ (C_{3v}^6). Relationships between their unit-cell parameter are obtained. The spontaneous polarization in these two phases is determined. The large thermal hysteresis of the transition is ascribed to the large structural change required at the transition.

I. INTRODUCTION

Lithium sodium niobate ($Li_xNa_{1-x}O_3$) are solid solutions based on sodium niobate ($NaNbO_3$) and lithium niobate ($LiNbO_3$). $LiNbO_3$ is an excellent ferroelectric and $NaNbO_3$ is antiferroelectric at room temperature. For the development of new ferroelectric and piezoelectric materials, an understanding of the phase diagram of the $Li_xNa_{1-x}NbO_3$ system is of primary importance. Although both $LiNbO_3$ and $NaNbO_3$ have NbO_6 octahedra as their basic structural units, they crystallize in different forms. $LiNbO_3$ at room temperature exhibits the "lithium niobate-type" structure with space group $R3c$ (C_{3v}^6),[1] while $NaNbO_3$ at room temperature has the perovskite structure with space group $Pbma$ (D_{2h}^{11}).[2] Because of this difference in crystal structure, single-phase solid solutions $Li_xNa_{1-x}NbO_3$ can be obtained only in the Na-rich region ($x \leq 0.17$)[3] or in the Li-rich region ($x \geq 0.95$).[4] Although $NaNbO_3$ shows ferroelectricity only below about 163 K,[5] $Li_xNa_{1-x}NbO_3$ have been found to be ferroelectric at room temperature for at least $x \geq 0.02$.[6] Around the composition $x = 0.12$, remarkably enhanced piezoelectric properties were observed.[7] Powder diffraction data revealed that the crystal structure at room temperature in the Li-rich region is a deformed $LiNbO_3$-type structure (rhombohedral),[8] and that in the Na-rich region it is orthorhombic for $x < 0.12$.[7] A "morphotropic phase boundary" between the orthorhombic and tetragonal phases thus exists at $x = 0.12$, which explains the enhanced piezoelectric properties near this composition.[9]

Available information on the phase relationship in the low-temperature range is scarce. Darlington and Megaw[2] determined the structure of the low-temperature phase of $NaNbO_3$, showing that its space group is $R3c$ (C_{3v}^6) below 143 K. Sadel *et al.*[6] claimed to have found evidence for a phase transition in a crystal with composition $x = 0.02$ by noting a very small peak in the dielectric constant at about 163 K. We studied the low-temperature properties of crystals in the composition range $x = 0.02$–0.16. Instead of a small peak in the dielectric constant ϵ we observed a large step of ϵ at low temperature with excellent reproducibility. Some preliminary results indicative of a phase transition have been reported.[10–12]

This paper presents our detailed investigation of the low-temperature phase transition of a crystal with composition $x = 0.03$. This particular composition was chosen because it has the orthorhombic symmetry to which most solid solutions (x up to 0.12) of this system belong. In addition, it is far enough away from the $NaNbO_3$ end point that it is ferroelectric at room temperature. In Sec. II is a brief description of the experimental procedure. Section III is devoted to the physical properties and the crystal structure, with the former including the dielectric constant, electrical resistivity, pyroelectric coefficient, spontaneous polarization, specific heat, and the thermal expansion. In Sec. IV, a summary and some conclusions are given.

II. EXPERIMENTAL PROCEDURE

The crystals of composition $x = 0.03$ used in this work were prepared by the Czochralski pulling technique in a MCGS-3 (Oxford Crystal Ltd) system. Typical growth conditions have been given in Ref. 13. Atomic absorption spectral analysis showed that the composition was $Li_{0.030\pm0.007}Na_{0.97\pm0.02}Nb_{1.00\pm0.02}O_3$. Room-temperature x-ray diffraction data revealed the crystal space group to be $Pc2_1b$ (C_{2v}^5).

a-axis-oriented, *b*-axis-oriented, and *c*-axis-oriented plates were cut from the crystal. For the dielectric constant, electrical resistivity, ferroelectric and pyroelectric measurements, the plates were of size about $5\times5\times0.4$ mm^3 with gold electrodes vacuum evaporated on the two major surfaces. Before the pyroelectric measurement, plates were poled in a dc electric field.

Spontaneous polarization was observed in the *b*-axis-

oriented plates (along the twofold axis b) at room temperature. It was measured by a TRC-1 quasistatic ferroelectric loop measuring instrument, the measuring frequency was 0.005 Hz.

The dielectric constant, dc electrical resistivity and the pyroelectric coefficient were measured in the temperature range from 20 to 300 K. The low-temperature facility was a DISPLEX low-temperature helium refrigeration system from the Air Products and Chemical, Inc. It consists of a CSW-202E microrefrigerator, a combined APD-E digital temperature indicator and controller and a DMX-15 interface. The system can be operated in the range of 300 to 10 K with temperature stability of 0.1 K. The dielectric constant was measured by a Hewlett-Packard 4192A type low-frequency impedance analyzer, the measuring frequency was 10 kHz. The dc resistivity was measured using a conventional circuit. The pyroelectric coefficient was measured by a charge integration technique with a Keithley 642 electrometer as the indicator.

A differential scanning calorimetric (DSC) study was performed in the temperature range from 100 to 300 K using a Perkin-Elmer DSC-2 type differential scanning calorimeter. Samples was c disks with 5-mm diameter and 1-mm thickness. Both the crystallization point and the fusion point of cyclohexane were used to calibrate the DSC-2 in terms of the temperature and the related heat of transition. Sapphire was used as the standard reference for the specific heat determination. Measurements were carried out in both the heating and the cooling processes with various rates of temperature variation.

The thermal expansion along the room temperature b axis was measured using a Perkin-Elmer TMS-2 type thermomechanical system. The measurement was carried out in the temperature range between 100 and 300 K.

III. RESULTS AND DISCUSSION

A. The dielectric constant and dc resistivity

Figure 1 shows the temperature dependence of the relative dielectric constant ϵ_{22}. The subscript 2 refers to the b axis which is the twofold axis and ferroelectric axis in the room-temperature phase. The arrows indicate the direction of the temperature change. It is seen that there is a large step in the dielectric constant and it has an extraordinarily large thermal hysteresis. In the cooling part of the cycle, the dielectric constant abruptly decreases at about 180 K while in the heating part of the cycle, it increases abruptly near 260 K.

We tested the reproducibility of the result in Fig. 1 in several ways: (1) alter the rate of temperature change between 2 K/min and 20 K/h; (2) make measurements on different samples; (3) repeat the experimental runs several times on the same sample. In each case, the curves in Fig. 1 were approximately reproduced. In particular, the two temperatures at which the dielectric constant rises or falls quickest were reproduced within ± 3 K.

The dielectric constant ϵ_{11} and ϵ_{33} were also measured in the same temperature range. Although the two values are different and not equal to ϵ_{22}, they have the same

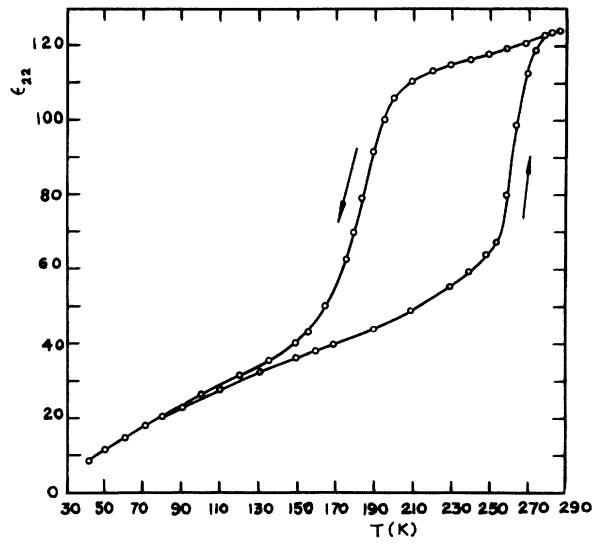

FIG. 1. Temperature dependence of the relative dielectric constant ϵ_{22}.

characteristics in their temperature dependence as ϵ_{22}, i.e., an abrupt decrease at about 180 K on cooling and an abrupt increase near 260 K on heating.

Figure 2 shows the temperature dependence of ρ_2, the dc electrical resistivity along the b axis. It is noted that ρ_2 also has a steplike behavior. It increases abruptly at about 180 K on cooling and decreases abruptly near 260 K on heating. Comparing Fig. 2 with Fig. 1, one can see that the increase in the resistivity corresponds to the decrease in the dielectric constant and vice versa.

B. Pyroelectric properties and the spontaneous polarization

Pyroelectricity is the manifestation of the change in electrical polarization, it should be a sensitive indicator of any phase transitions in which the polarization changes. Shown in Fig. 3 is the pyroelectric coefficient

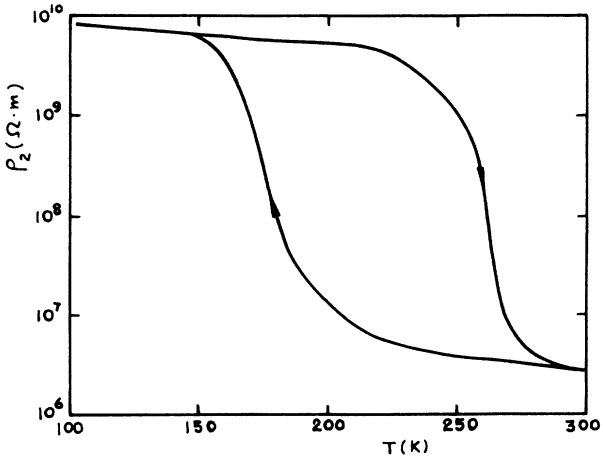

FIG. 2. Temperature dependence of the dc electrical resistivity along the room-temperature b axis.

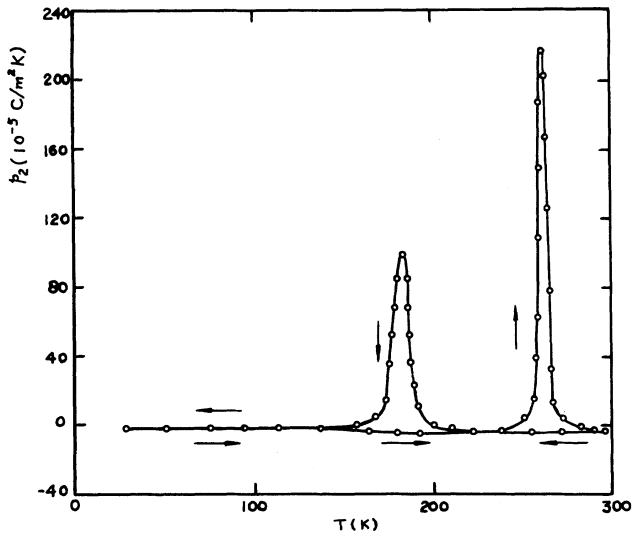

FIG. 3. Temperature dependence of the pyroelectric coefficient p_2.

measured along the b axis. Two peaks are conspicuous in the figure: One appears at about 180 K on cooling; the other appears near 260 K on heating. These two temperatures are approximately the same as those at which the dielectric constant and the dc resistivity jump. The jump at about 260 K is higher and sharper than that at about 180 K. The former has a peak value of 2.15×10^{-3} C/m^2 K and the latter is 1.05×10^{-3} C/m^2 K. Apart from the two positive peaks, the values of p_2 are very small and negative. Measurements were made using different samples and on the same sample with various rates of temperature change. The reproducibility of the curve in Fig. 3 was fairly good, in particular, the temperatures at which the p_2 peaks were reproduced within ±4 K.

The spontaneous polarization at room temperature was measured to be 2.52×10^{-2} C/m^2. It lies along the twofold axis as is expected from the symmetry restriction by the point group $m2m$ (C_{2v}). Using the room-temperature spontaneous polarization and integrating the pyroelectric coefficient p_2 over T, one can obtain the spontaneous polarization as a function of temperature. The result is shown in Fig. 4. It is seen that an abrupt change occurs at about 180 or 260 K depending on the direction of the temperature variation. When the temperature is higher than 280 K or lower than 120 K, the polarization increases with decreasing temperature monotonically. The p_2 at low temperature is much less than that at room temperature; in particular, it is 1.55×10^{-2} C/m^2 when $T=50$ K. Approximately the same value was obtained by measuring the ferroelectric loops.

The anomalies in the dielectric constant, dc resistivity, pyroelectric coefficient, and the spontaneous polarization suggest a phase transition. It is between two ferroelectric phases, since ferroelectric loops were observed in the low-temperature phase as well as at room temperature.

At a transition between two ferroelectric phases, the polar axis may be rotated or remain in the same direction. To know which is true in the present case, some a-axis-oriented plates and c-axis-oriented-plates were exam-

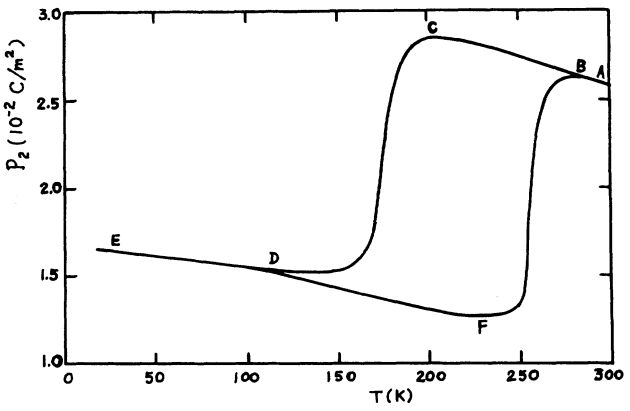

FIG. 4. Temperature dependence of the spontaneous polarization along the room-temperature a axis.

ined. A dc electric field was applied to an a-axis-oriented plate or c-axis-oriented plate at room temperature, then the sample was cooled with the electric field maintained. When the temperature was lower than 20 K, the electric field was removed. After this, the sample was heated and a measurement was made to test whether it is pyroelectric. For the c-axis-oriented plates, no pyroelectricity was detected. It means that the spontaneous polarization does not have component along the c axis till 20 K. On the other hand, a pyroelectric effect was observed in the a-axis-oriented plates. Figure 5 shows the measured pyroelectric coefficient p_1 as a function of temperature. $p_1\neq0$ implies that the polar axis changes its direction at the transition. At room temperature a axis is perpendicular to the polar axis (b axis). If the polar axis did not change its direction, there could not be any component of the spontaneous polarization along the a axis at low temperature as well. Therefore, the appearance of p_1 must be due to a rotation of the polar axis.

To obtain the a-axis component of the spontaneous polarization in the low-temperature phase, P_1, the pyroelec-

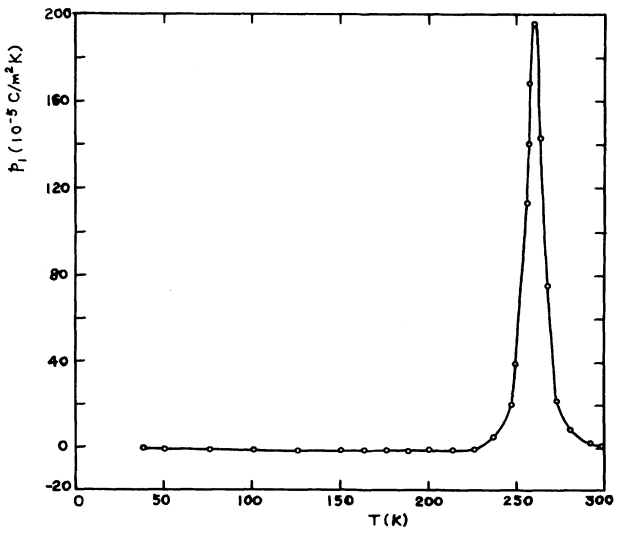

FIG. 5. Temperature dependence of the pyroelectric coefficient along the room-temperature a axis.

tric coefficient p_1 was integrated over temperature T. This gave $P_1 = 2.15 \times 10^{-2}$ C/m^2 at $T = 50$ K.

Up to now, we have obtained the three components of the spontaneous polarization in the low-temperature phase. When $T = 50$ K, $P_1 = 2.15 \times 10^{-2}$ C/m^2, $P_2 = 1.55 \times 10^{-2}$ C/m^2, $P_3 = 0$. Thus we know that the spontaneous polarization at this temperature has a value of 2.65×10^{-2} C/m^2 and is in the ab plane and at an angle of θ with the b axis, where $\theta = \tan^{-1}(2.15/1.55) = 54.2°$.

C. Specific heat and the thermal expansion

Further evidence of the phase transition is provided by the specific-heat anomaly and the thermal expansion behavior. From the DSC measurement with a heating rate of 5 K/min, the specific heat was obtained and is shown in Fig. 6(a). It is seen that a sharp peak appears at about 260 K. Since the spontaneous polarization changes drastically at this temperature, the peak in the specific heat must be due to the energy associated with the change in the spontaneous polarization. Integrating the area under this peak we can obtain the heat of transition ΔQ and the change in entropy at the transition $\Delta S = \Delta Q/T$. The results are $\Delta Q = 212 \pm 50$ J/mol, $\Delta S = 0.82$ J/mol K.

DSC measurement with a cooling rate of -5 K/min resulted in the specific heat curve in Fig. 6(b). It is noted that a peak appears at about 180 K. Comparing Fig. 6(a) with 6(b) one can see that the peak has a thermal hysteresis of about 80 K. Integrating the area under the peak in Fig. 6(b) we obtained the heat of transition ΔQ. As is expected the value equals that obtained in the process of heating within error.

It is also interesting to note that the peak in Fig. 6(b) is not so sharp as that in Fig. 6(a). This is consistent with the pyroelectric behavior. As is seen in Fig. 3, the pyroelectric coefficient peak obtained on cooling is broader than that on heating. These imply that the transition accomplishes in a narrower range on heating than on cooling.

The thermal expansion along the room-temperature b axis is shown in Fig. 7. It was obtained with a temperature variation rate of 5 K/min (heating) and -5 K/min (cooling). In the process of cooling, the sample abruptly contracts at about 180 K; in the process of heating, it expands abruptly at 260 K. These two temperatures coincide with those at which the electric and thermal properties anomalously change. All the anomalies are therefore manifestations of the same transition—a phase transition with thermal hysteresis of about 80 K.

D. The crystal structure and the phase transition

The crystal structure at room temperature (290 K) was first studied. The space group was determined to be $Pc2_1b(C_{2v}^5)$, which is the same as that of $x = 0.02$ reported by Von Der Mühll, Sadel, and Hagenmuller.[14] The cell parameters are $a = 5.523(8)$ Å, $b = 15.564(9)$ Å, $c = 5.556(7)$ Å.

The crystal structure was then investigated at about 130 K. Oscillation photographs were first taken around the room-temperature symmetry axes. The unit cell seemed to be simply half of that at room temperature

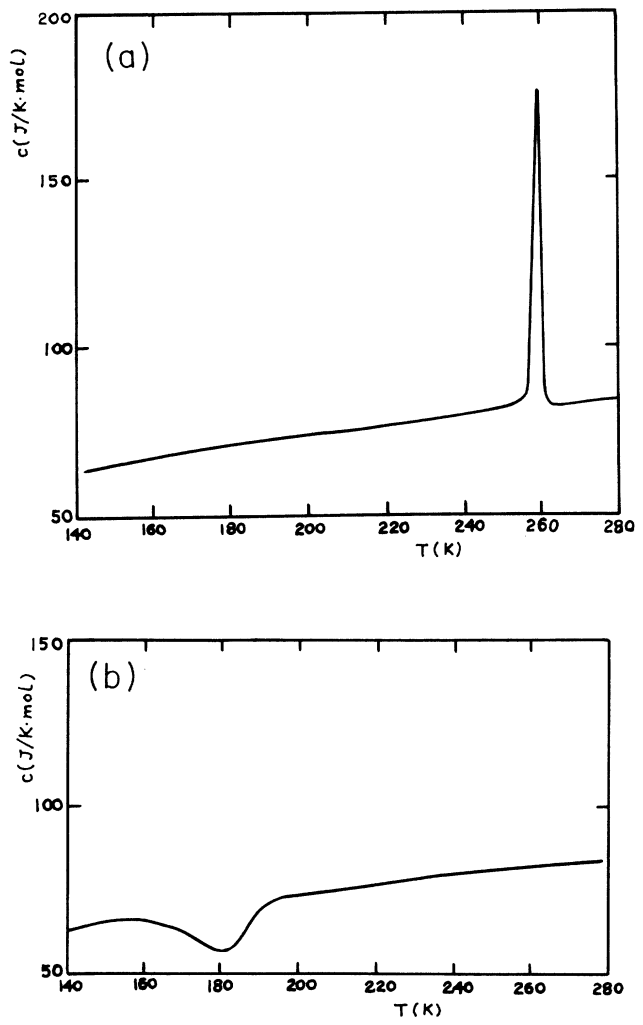

FIG. 6. Temperature dependence of the specific heat on heating (a) and cooling (b).

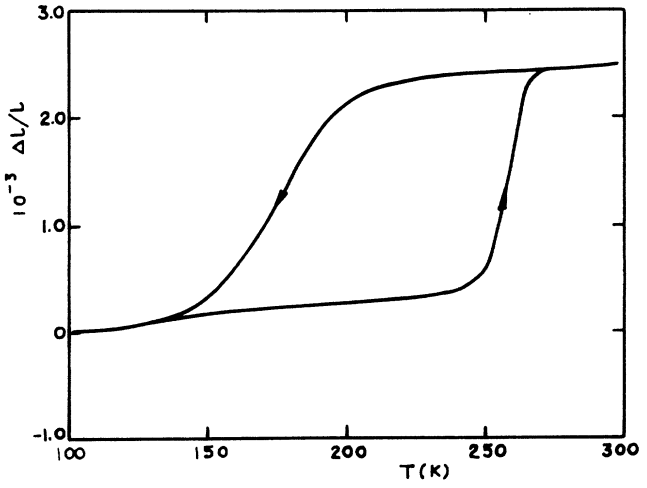

FIG. 7. The thermal expansion along the room-temperature b axis.

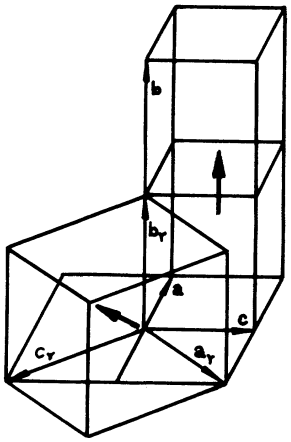

FIG. 8. The relation between the unit-cell parameter of the RT phase and that of the LT phase. **a**, **b**, **c**, and $\mathbf{a}_r$, $\mathbf{b}_r$, $\mathbf{c}_r$ are cell edges in the RT phase and the LT phase, respectively. The thick arrows indicate the spontaneous polarization.

with the b axis shortened by half. However, calculation and refinement of the unit-cell parameter and orientation matrix showed it was no longer orthorhombic but rhombohedral with cell parameters $a_r=b_r=c_r=7.811(12)$ Å, $a=\beta=r=89°23'$ (5). Because the cooling system occupied considerable space, the measured reflections were limited. Although they were not enough to obtain the atom positions, the reflection conditions hhl (with $1=2n$) and hhh (with $h=2n$) were obeyed. In addition, the relationship $I(hkl)=I(lhk)=I(klh)$ was also observed. Thus the space group should be $R3c$ (C_{3v}^6).

The relationship between the unit-cell parameter in the room-temperature (RT) phase and those in the low-temperature (LT) phase can be approximately described as follows (see Fig. 8):

$$\mathbf{a}_r=-\mathbf{a}+\mathbf{c},\quad \mathbf{b}_r=\mathbf{b}/2,\quad \mathbf{c}_r=-\mathbf{a}-\mathbf{c}\ .$$

Because the point group of the low-temperature phase is $3m$ (C_{3v}^6), the spontaneous polarization must be along the threefold axis (in the body diagonal direction of the rhombohedral cell), that is, at an angle of approximately 54.7° with any of the a_r, b_r (or b), and c_r axes. In Sec. III B we have obtained the angle between the spontaneous polarization and the b axis to be 54.2°. These two values are in fairly good agreement with each other.

The unit-cell volume at room temperature (290 K) is 477.6 Å^3 and that in the low-temperature phase ($T=50$ K) is 476.4 Å^3. This is consistent with the contraction on cooling and the expansion on heating show in Fig. 7.

The structural change at the transition is large as can be seen in Fig. 8. It can account for the large thermal hysteresis of the transition.

IV. SUMMARY AND CONCLUSIONS

In this paper we have studied the physical properties and the crystal structure of a crystal with composition $Li_{0.03}Na_{0.97}NbO_3$ prepared by use of the Czochralski technique. Through this study we have detected a low-temperature phase transition in this crystal.

The dielectric constant, dc electrical resistivity, pyroelectric coefficient, spontaneous polarization, specific heat, and the thermal expansion have been measured in a wide temperature range below 300 K. The pyroelectric coefficient and specific heat exhibit a peak at about 180 K on cooling and 260 K on heating. The dielectric constant, dc electrical resistivity, spontaneous polarization, and the thermal expansion abruptly decrease or increase at about 180 or 260 K depending on the direction of the temperature change, resulting in a large step around these two temperatures. These are indicative of a phase transition which occurs at about 180 K on cooling and near 260 K on heating.

X-ray diffraction experiment has been performed on the crystal at room temperature (290 K) and at about (130 K). From this, the space group and the unit-cell parameters of the room-temperature phase and the low-temperature phase are obtained, the relationship between the unit-cell parameters of these two phases has been determined.

Both the room-temperature phase and the low-temperature phase are ferroelectric. The spontaneous polarization at room temperature (290 K) and $T=50$ K are 2.52×10^{-2} C/m^2 and 2.65×10^{-2} C/m^2, respectively. On undergoing the transition, the spontaneous polarization changes its direction from the room-temperature twofold axis to the low-temperature threefold axis, turning through an angle of about 54°.

The transition is a first order one. The thermal hysteresis of the transition is about 80 K, which can be attributed to the large structural change required at the transition.

ACKNOWLEDGMENTS

We wish to thank Professor R. Von Der Mühll of the university of Bordeaux I for his help in the work. We acknowledge the support from the Science Fund of the Chinese Academy of Sciences.

[1]S. C. Abrahams, W. C. Hamilton, and J. M. Raddy, J. Chem. Phys. Solids **27**, 1013 (1966); **27**, 1019 (1966).
[2]C. N. W. Darlington and Helen D. Megaw, Acta Crystallogr. B **29**, 2171 (1973).
[3]R. Von Der Mühll *et al.*, Solid State Commun. **31**, 151 (1979).
[4]H. W. Grueninger, R. R. Zeyfang, and M. Gauntlett, Ber. Dtsch. Keram. Ges. **52**, 238 (1975).
[5]L. E. Cross and B. J. Nicholson, Philos. Mag. **46**, 453 (1955).
[6]A. Sadel *et al.*, Ferroelectrics **47**, 169 (1983).
[7]R. M. Henson, R. R. Zeyfang, and K. V. Kiehl, J. Amer. Ceram. Soc. **60**, 15 (1977).
[8]H. W. Grueninger, R. R. Zeyfang, and C. P. Reeves, Ferroelectrics **11**, 413 (1976).
[9]Y. Y. Song *et al.*, Synthetic Crystals (in Chinese) **18**, 117 (1989).
[10]P. L. Zhang *et al.*, Solid State Commun. **67**, 1215 (1988).
[11]Zhong Weilie *et al.*, Ferroelectrics **101**, 261 (1990).
[12]C. L. Wang *et al.*, J. Appl. Phys. **69**, 2522 (1991).
[13]P. L. Zhang *et al.*, Jpn. J. Appl. Phys. **24**, Suppl. 24-2, 998 (1985).
[14]R. Von Der Mühll, A. Sadel, and P. Hagenmuller, J. Solid State Chem. **51**, 176 (1984).